

Preliminary investigation on the adoption of CO₂-SO₂ working mixtures in a transcritical Recompression cycle

Francesco Crespi*, Pablo Rodríguez de Arriba, David Sánchez, Antonio Muñoz

University of Seville, Camino de los descubrimientos s/n, 41092 Seville, Spain.

Abstract

This paper investigates the interest and potential of using working fluids based on Carbon and Sulphur Dioxide mixtures (CO₂-SO₂) in a transcritical *Recompression* cycle. In order to assess the actual thermodynamic potential of the concept proposed, the influence of dopant (SO₂) content is assessed for two different turbine inlet temperatures (550°C and 700°C). The results obtained are compared with other CO₂ mixtures already proposed in literature (CO₂-C₆F₆ and CO₂-TiCl₄) and for two alternative cycle layouts (*Recuperated Rankine* and *Precompression*).

The results of the analysis reveal that, at high ambient temperature, the *Recompression* cycle operating on CO₂-SO₂, with Sulphur Dioxide content between 20% and 30%(v), is a very interesting option for Concentrated Solar Power plants, able to achieve thermal efficiencies $\approx 45\%$ and $>51\%$ at 550°C and 700°C respectively. At a minimum cycle temperature of 50°C, the proposed configuration leads to thermal efficiency gains of 6% and 2% with respect to the *Brayton* and *Recompression* cycles working on pure CO₂. This performance enhancement of the *Recompression* cycle with CO₂-SO₂ is comparable to or higher than that enabled by other CO₂ mixtures proposed in literature, but with significantly higher specific work (smaller footprint) and temperature rise across the solar receiver (lower installation costs).

Keywords: Supercritical Carbon Dioxide, Power cycle, Mixture, Thermodynamic, Recompression, Sulphur Dioxide

1. Introduction

The scientific community and industry agree on the potential of Supercritical Carbon Dioxide (sCO₂) cycles for next generation CSP plants, owing to their high thermal efficiency and arguably smaller footprint. The growing interest in this technology can be monitored through the large number of publications on the topic produced in the last fifteen years. These have discussed aspects of the technology such as thermodynamic assessment of cycles [1, 2], aerothermal and mechanical design of components [3–5], system integration [6–8] and economic analysis [9, 10].

*Corresponding author. Tel.: +34 954 482 005.

Email addresses: cresp@us.es (Francesco Crespi), prdearriba@us.es (Pablo Rodríguez de Arriba), ds@us.es (David Sánchez), amb1@us.es (Antonio Muñoz)

7 Nevertheless, the technology is also acknowledged to have a critical weakness stemming from the need to carry out
8 compression near the critical point of CO₂ (31.04°C, 73.88 bar), in order to unleash the thermodynamic potential of
9 these cycles. When this is not the possible, for instance due to high ambient temperatures (usual in CSP applications),
10 compressor inlet temperature increases and the thermal performance of sCO₂ power systems drops dramatically. This
11 is inherent to the properties of Carbon Dioxide and cannot be compensated for by the adoption of advanced layouts
12 which, in addition to not solving the problem, are very likely to increase installation costs prohibitively [11].

13
14 In order to solve this problem, several authors have investigated the utilisation of working fluids based on CO₂
15 mixtures where certain chemical compounds are added to the raw CO₂ flowing in the system: Invernizzi and Van der
16 Stelt [12], and recently Siddiqui [13], explore the potential of mixtures based on CO₂ and hydrocarbons; Baik and Lee
17 provide a preliminary analysis of the potential of CO₂-R32 mixtures using experimental data [14]; and Manzolini *et*
18 *al.* [15] present a techno-economic assessment of cycles using this concept in Concentrated Solar Power applications.

19
20 The SCARABEUS project, funded by the Horizon 2020 programme of the European Commission [16], follows
21 this pathway. In this project, the addition of certain dopants to Carbon Dioxide yields a mixture with higher critical
22 temperature than pure CO₂, enabling compression of the working fluid close to its critical temperature even in hot
23 environments ($T_{a,b} \approx 50^\circ\text{C}$) [17, 18]. The concept will be demonstrated experimentally at a dedicated rig during the
24 project.

25
26 Previous works by the authors of this paper, within the context of the SCARABEUS project, investigated the
27 thermal performance gains enabled by mixtures of Carbon Dioxide and Titanium Tetrachloride (TiCl₄) or Hexaflu-
28 orebenzene (C₆F₆) in power cycles [18–20]. A thorough literature review of supercritical cycles, with emphasis on
29 transcritical condensing cycles, showed that the *Recuperated Rankine* and *Precompression* layouts were able to fully
30 exploit the potential of CO₂-TiCl₄ and CO₂-C₆F₆ mixtures respectively. These results are expanded to mixtures of
31 CO₂ and Sulphur Dioxide (SO₂) in this paper, with the aim to identify i) the potential for performance enhancement
32 enabled by this dopant, and ii) the cycle layout yielding larger performance gains. As shown later in the paper, it is
33 observed that the *Recompression* cycle achieves very good performance with this mixture and, therefore, it is added
34 to the *Recuperated Rankine* and *Precompression* layouts for a detailed analysis.

35
36 This is the first time a transcritical *Recompression* cycle using CO₂-SO₂ mixtures is presented in literature, to
37 the authors' best knowledge, although partly related works must be acknowledged. Tafur-Escanta *et al.* investigated
38 four different CO₂-based mixtures, including 90%CO₂-10%SO₂ in a supercritical *Recompression* power cycle cou-
39 pled to a solar thermal parabolic-trough plant, concluding that CO₂-SO₂ mixtures could improve cycle efficiency by
40 3% [21]. Wang *et al.* presented a similar approach, considering different dopants in either *Recuperated Brayton* or
41 *Recompression* cycles, and found that adding 5% SO₂ in a *Recompression* cycle could increase thermal efficiency by

42 about 2% with respect to the same layout with pure CO₂ [22]. Rath *et al.* also considered SO₂ in a wide analysis
43 of the *Simple Recuperated* cycle operating on CO₂ mixtures with 135 different dopants [23]. The authors found that
44 only marginal gains in terms of thermal efficiency (<1%) were possible with respect to the same cycle using pure
45 CO₂. Finally, another paper developed in the framework of the SCARABEUS project and authored by Aqel *et al.*
46 has recently looked into the impact that using CO₂ mixtures with SO₂, TiCl₄ and C₆F₆ has on turbine design for a
47 *Recuperated Rankine* cycle [24].

48

49 Based on this past work by the same and other authors, the paper is organised as follows. In the first part of the
50 paper, a brief characterisation of Sulphur Dioxide is provided, along with a discussion regarding the main features
51 of CO₂-SO₂ mixtures. Then, the thermal performances enabled by transcritical *Recompression* cycles operating on
52 this non-conventional fluid are assessed, considering two different turbine inlet temperatures (550°C and 700°C) and
53 comparing the results with other layouts (*Recuperated Rankine* and *Precompression*) and dopants (C₆F₆, TiCl₄).
54 Finally, a comparison of the foregoing cases against a *Recompression* cycle using pure CO₂ is presented in order to
55 investigate the actual applicability and potential of the concept proposed in the paper.

56 2. Characterisation of Sulphur Dioxide and definition of candidate mixtures

57 Sulphur Dioxide is a colourless gas widely employed in the industry for applications such as food preservation
58 (antiseptic) or refrigeration [25, 26]. Characterised by a pungent odour, SO₂ is produced both naturally (volcanic
59 eruptions) or via anthropogenic activity, primarily combustion of fossil fuels (coal and oil) and smelting of minerals
60 containing sulphur (copper, lead) [27]. It presents high solubility in several organic solvents, extremely high thermal
61 stability and it is neither explosive nor flammable [28]. On the other hand, the compound is highly irritant and clas-
62 sifies as Level 3 for health hazard according to NFPA-704 standards [29] and safety group B1 by ASHRAE [30].
63 When inhaled, usual symptoms range from nasal inflammation to bronchoconstriction but there is limited evidence of
64 chronic toxicity, generally similar to chronic bronchitis without the involvement of bacterial infection [31].

65

66 The characteristics of the dopants considered in the SCARABEUS project are presented in Table 1, based on the
67 NFPA-704 standard. Other refrigerants and thermal oils are also listed in the Table for the sake of comparison. It is
68 observed that Sulphur Dioxide exhibits less safety-related issues and better reliability than other dopants considered
69 in earlier phases of the project: Hexafluorobenzene (C₆F₆, high flammability) or Titanium Tetrachloride (TiCl₄, high
70 water reactivity). The health hazard characteristics of SO₂ are similar to those of Therminol VP-1 (widely employed
71 in Concentrated Solar Power plants using parabolic-trough technology), and significantly safer than Ammonia, a very
72 common refrigerant classified as B2L according to ASHRAE. Similarly, other state-of-the-art refrigerants such as
73 propane (R-290) or R-1234yf, common in air-conditioning and refrigeration systems, exhibit values comparable to
74 those of SO₂ in the NFPA-704 classification system.

Table 1: Hazards of different fluids according to NFPA 704 [29].

	Health Hazard	Flammability	Chemical Reactivity	Special Hazard
CO ₂	2	0	0	Simple Asphyxiant
SO ₂	3	0	0	-
C ₆ F ₆	1	3	0	-
TiCl ₄	3	0	2	Reacts with water
Ammonia	3	3	0	-
R-290	2	4	0	-
R-1234yf	1	4	0	-
Therminol 66	1	1	0	-
Therminol VP-1	2	1	0	-

75 It is worth noting that the characteristics of Sulphur Dioxide are not far from those of CO₂, which is a simple
 76 asphyxiant gas classifying as Level 2 for health hazard, and these similarities extend to the thermodynamic features of
 77 the compounds. In particular, Table 2 shows that both SO₂ and CO₂ present very high thermal stability -significantly
 78 higher than C₆F₆ or TiCl₄- and very similar critical pressure and molecular complexity*.

Table 2: Thermodynamic properties of Carbon Dioxide and the three dopants considered in the SCARABEUS project.

	MW [kg/kmol]	T _{cr} [°C]	P _{cr} [bar]	Molecular Complexity [-]	Thermal Stability
CO ₂	44.01	31.06	73.83	-9.324	>700°C [28]
SO ₂	64.06	157.60	78.84	-8.230	>700°C [28]
C ₆ F ₆	186.06	243.58	32.73	12.740	up to 625°C †
TiCl ₄	189.69	364.85	46.61	1.922	up to 700°C [33]

79 A concern about using CO₂-SO₂ mixtures in supercritical power cycles is the risk to experience corrosion pro-
 80 moted by SO₂ on wet metal surfaces [34, 35], as a consequence of the creation of sulphuric acid (H₂SO₄) when SO₂
 81 reacts with water. This is currently under investigation in oxycombustion applications which naturally contain traces
 82 of SO₂ and a substantial amount of H₂O as a consequence of combustion (for instance, the *Allam* cycle [36]). In
 83 Concentrated Solar Power applications operating on CO₂-SO₂ mixtures, there is no water formation because there is
 84 no combustion. This mitigates this risk to experience corrosion.

85
 86 It is worth noting that the corrosion problem presented in the foregoing is different from that experienced in pure

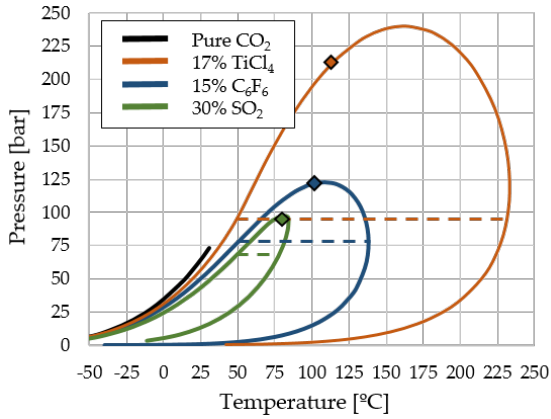
*The molecular complexity has been estimated as $(T_c/R) \cdot (dS/dT)_{T_R=0.7}$, see page 109 in reference [32].

†Threshold temperature obtained by University of Brescia and Politecnico di Milano for the SCARABEUS project. Complete set of experi-
 mental results to be disclosed in a future publication by these two institutions.

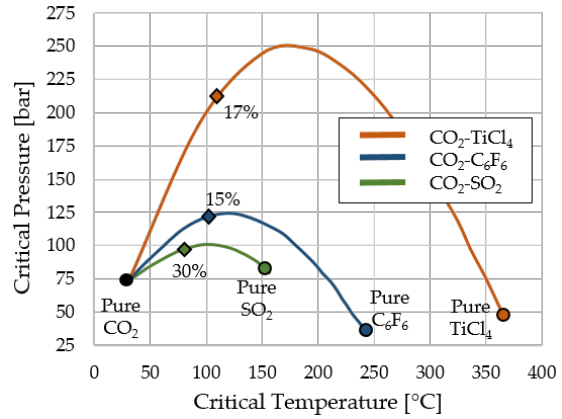
87 CO₂ applications, which is caused by material oxidation and observed even with advanced alloys [37–39]. This latter
88 phenomenon is nevertheless applicable to either pure CO₂ or CO₂ mixtures and does not constitute a problem specific
89 to supercritical power systems operating on sCO₂ mixtures. Moreover, the onset and severity of corrosion is a com-
90 plex problem that falls out of the scope of the paper; hence, it is not discussed here.

91
92 The thermophysical properties of CO₂-SO₂ mixtures are calculated with Aspen Properties v11.0, using a standard
93 Peng-Robinson Equation of State (PR EoS), calibrated on experimental data of the corresponding Vapour-Liquid-
94 Equilibrium (VLE) conditions [40]. This dataset is provided by University of Brescia and Politecnico di Milano,
95 partners of the SCARABEUS consortium, who also worked on identifying SO₂ as a potential dopant. It is to note that
96 the behaviour of the mixture has been estimated with other models, in addition to the standard PR EoS: copolymer
97 PC-Saft model (PC-SAFT), Lee-Kleser Plocker (LK-Plock) and Nist-REFPROP method. The results of this assess-
98 ment, to be disclosed soon in publication by the aforementioned institutions, reveal that using PR and PC-Saft yields
99 the best match to the experimental and literature data available, even if with slight differences: PR yields a better
100 estimate of the critical pressure and temperature of the mixture whilst PC-Saft seems to be the best option for an
101 overall assessment of the thermophysical properties of the mixtures, in particular when speed of sound and residual
102 heat capacity are relevant. These parameters are of utmost importance for the thermo-mechanical design of cycle
103 components, especially turbomachinery, but their effect on the preliminary assessment of cycle performance is very
104 weak. More information about this latter influence is provided in [Appendix A](#) of the present manuscript, where
105 using different EoS is proved to bring about thermal efficiency variations lower than 1.5% (≈ 0.6 percentage points
106 in absolute terms), regardless of the dopant content and operating temperatures of the cycle. Therefore, for the sake
107 of simplicity and consistence with previous works by the authors, the standard PR Equation of State is used in the
108 present manuscript.

109
110 In previous studies by the authors of this paper [18], the minimum molar fraction of dopant was set to yield a
111 critical temperature of the mixture of $\approx 80^\circ\text{C}$. This value provides a 30°C gap between the minimum cycle tempera-
112 ture (T_{min} , set to 50°C for the reference case in a hot environment) and the critical temperature of the working fluid
113 (T_{cr}), thus enabling condensation even in the most adverse conditions (i.e., highest ambient temperature). This yields
114 minimum molar fractions of 10% and 14% when using C₆F₆ and TiCl₄ respectively, values that are lower than the
115 optimum dopant content for peak thermal efficiency (see Table 3). For Sulphur Dioxide, the same constraint corre-
116 sponds to a minimum molar fraction of 30%SO₂, significantly higher than for the other compounds. This is due to the
117 substantially lower critical temperature of SO₂, see Table 2, affecting the Pressure-Temperature (p - T) envelopes and
118 the critical loci of the mixtures. A graphical description of this is provided in Figure 1(a), where a 70%CO₂-30%SO₂
119 mixture is compared to 85%CO₂-15%C₆F₆ and 85%CO₂-15%TiCl₄, the two mixtures yielding the best cycle perfor-
120 mance with Hexafluorobenzene and Titanium Tetrachloride respectively [18]. The case for pure CO₂ is also shown
121 for comparison. The effect of composition on the shape of p - T envelopes for the three dopants is visible, both in terms



(a) Pressure-Temperature envelopes for different SCARABEUS mixtures.



(b) Critical Loci of the three dopants considered.

Figure 1: Pressure-Temperature envelopes for three different mixtures and pure CO₂ (left) and critical loci for the three dopants (right). In Figure (a), critical points are represented by markers while temperature glides for a bubble temperature of 50°C are indicated with dotted lines.

122 of position of the critical point and width of the envelope. This last aspect, also called temperature glide (dashed lines
 123 in Figure 1(a)), is proportional to the difference between the critical temperature of Carbon Dioxide and the critical
 124 temperature of the dopant, and it is crucial for the feasibility of some supercritical CO₂ cycles operating on mixtures
 125 (this is explained further in the last section of the paper).

126
 127 Further to the foregoing discussion, Carbon Dioxide mixtures with Sulphur Dioxide have a very relevant difference
 128 with both CO₂-C₆F₆ and CO₂-TiCl₄. For the latter two mixtures, the dopant fractions (of C₆F₆ and TiCl₄) yielding
 129 peak cycle efficiency have critical temperatures higher than 80°C. This is however not the case for SO₂, whose opti-
 130 mum SO₂ fraction efficiency-wise is lower than 30% (it is reminded here that a 70/30 CO₂-SO₂ mixture has a critical
 131 temperature of ≈80°C). This means that the 30°C temperature gap (ΔT_{gap}) between minimum cycle temperature and
 132 critical temperature of the mixture is actually constraining the design space of the cycle in the quest for higher ef-
 133 ficiencies. In the light of this, and in order to explore potential efficiency gains beyond this constraint, it is decided
 134 to reduce the minimum molar fraction of SO₂ allowed to 20%, which corresponds to a ΔT_{gap} of about 15°C. The
 135 characteristics of three representative mixtures with 20, 30 and 40%(v) SO₂ content are summarised in Table 3 along
 136 with those of the optimum mixtures with TiCl₄ and C₆F₆ (peak cycle efficiency). As usual, the following standard
 137 code is used to label each mixture: DxCyy, where x identifies the dopant (1=C₆F₆, 2=TiCl₄, 3=SO₂) and yy represent
 138 the corresponding molar fraction.

Table 3: Main characteristics of working fluids. P_{cond} and temperature glide refer to a bubble temperature of 50°C.

Mixture	Molar Comp. [%]	MW [kg/kmol]	T_{cr} [°C]	P_{cr} [bar]	P_{cond} [bar]	Glide [°C]
D1C15	CO ₂ -C ₆ F ₆ [85-15]	65.32	102.1	121.3	77.52	88.4
D2C17	CO ₂ -TiCl ₄ [83-17]	68.77	116.4	212.6	96.17	181.6
D3C20	CO ₂ -SO ₂ [80-20]	48.03	64.2	91.85	77.41	16.1
D3C30	CO ₂ -SO ₂ [70-30]	50.03	79.47	97.51	68.53	27.99
D3C40	CO ₂ -SO ₂ [60-40]	52.03	93.79	100.5	60.12	38.55

3. Computational environment and cycle modeling

The system has been modelled with Thermoflex v.29, a commercial software developed by Thermoflow Inc. [41], with the thermophysical properties of the working mixtures incorporated in the form of look-up tables. These look-up tables have been produced with Aspen by University of Brescia and Politecnico di Milano [42] and then added to Thermoflex through *User-defined fluid* tool specifically developed by Thermoflow for the SCARABEUS project. At this preliminary stage, the main cycle components (heat exchangers and turbomachinery) are modelled with lumped-volume models already built into the software.

The specifications of the reference power block are summarised in Table 4. Gross power output is set to 100MW whilst two different turbine inlet temperatures are considered: 550°C, corresponding to state-of-the-art tower-type CSP plants, and 700°C, representative of next-generation receiver technology. The effects of varying minimum cycle temperature, isentropic efficiency of turbomachinery and minimum temperature difference of recuperators are investigated as well, considering values in the following ranges respectively: 30°C-60°C, 80-100% and 5-25°C.

Table 4: Boundary conditions and specifications of turbomachinery and heat exchangers.

PIT [°C]	TIT [°C]	P_{max} [bar]	η_{is} [%]	ΔT_{min} [°C]	ΔP_{heater} [bar]	ΔP_{cond} [bar]	ΔP_{rec} [%]
			Pump/Turb/Compr				Low P / High P
50	550/700	250	88 / 93 / 89	5	1.5	0	1 / 1.5

Three cycle layouts are considered, whose schematic representations are shown in Figure 2: *Recuperated Rankine*, *Precompression* and *Recompression* [43]. The two first layouts, *Recuperated Rankine* and *Precompression*, are the most interesting options for CO₂-TiCl₄ and CO₂-C₆F₆ mixtures as credited in previous works by the authors [18]. On the other hand, the *Recompression* cycle is very likely the most well-known sCO₂ cycle and has been investigated widely in literature. Here, the cycle is adopted in a transcritical embodiment, in order to exploit the potential of CO₂-SO₂ mixtures in condensing cycles.

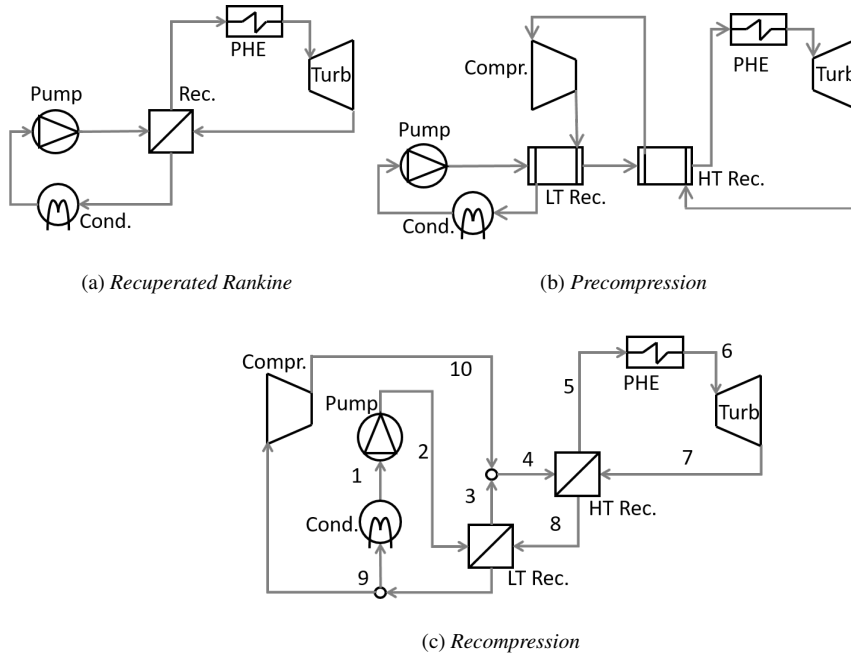


Figure 2: Cycle layouts considered in the analysis.

4. Discussion of results

4.1. Best-performing mixture and layout

The thermal performance of the three cycles considered, as a function of the molar content of SO_2 , is presented in Figure 3. Thermal efficiency (η_{th}) and specific work (W_s) are the main figures of merit while the inlet temperature to the Primary Heat Exchanger (PHE) and turbine outlet pressure are complementary parameters of interest. As indicated in the legend, the blue, orange and green lines correspond to the *Recuperated Rankine*, *Precompression* and *Recompression* cycles respectively. For all these cases, dashed lines apply to a turbine inlet temperature of 550°C and solid lines to 700°C .

A first observation in Figure 3(a) is the monotonically decreasing trend of thermal efficiency for increasing SO_2 concentration, with a slope that depends weakly on cycle configuration and is similar for both turbine inlet temperatures considered. In a closer look, the *Precompression* cycle at 700°C presents the largest slope, changing from 47.1% for 20% SO_2 (D3C20) to 45.7% for 40% SO_2 (D3C40), whilst the thermal efficiency of the *Recuperated Rankine* cycle operating at 550°C remains approximately constant regardless of the molar fraction of SO_2 (thermal efficiency varies by 0.4 percentage points in the range under analysis). Specific work presents the opposite trend, increasing in parallel with the molar fraction of Sulphur Dioxide, Figure 3(b). Relative variations of this figure of merit range from 8.6% (*Recompression* cycle at 700°C) to 13% (*Recuperated Rankine* cycle at 700°C).

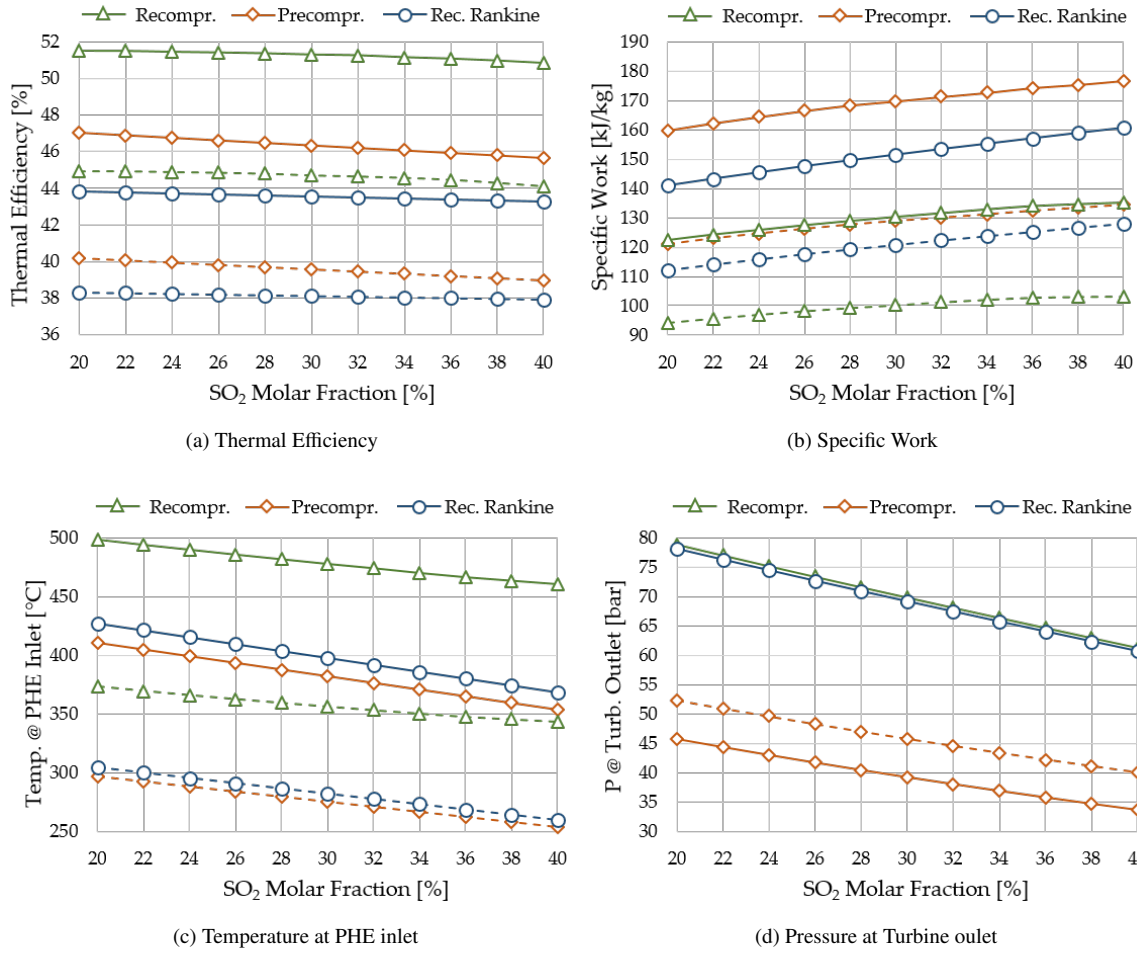


Figure 3: Influence of SO₂ content on the performance of transcritical cycles working on CO₂ mixtures. Dashed lines correspond to TIT=500°C. Solid lines correspond to 700°C.

176 Figure 3 also confirms that the *Recompression* cycle is very interesting when CO₂-SO₂ mixtures are used. For a
 177 turbine inlet temperature of 550°C, this configuration yields $\eta_{th} \approx 45\%$, whilst the *Recuperated Rankine* and *Precom-*
 178 *pression* layouts hardly achieve 38.5% and 40.5% respectively. Moreover, this superior performance of the *Recom-*
 179 *pression* cycle is so clear that it achieves similar efficiency at 550°C than the other cycle layouts at 700°C. This puts the
 180 *Recompression* cycle operating at 550°C forward as a very interesting alternative for CSP applications, achieving ther-
 181 mal efficiencies higher than subcritical or even supercritical steam turbines using state-of-the-art receiver technology
 182 ($\approx 42\%$, for a minimum cycle temperature of 50°C [18]). At 700°C, the *Recompression* cycle on a 70%CO₂/30%SO₂
 183 mixture outperforms both *Precompression Recuperated Rankine* by a margin larger than 5 percentage points efficiency
 184 wise.

185
 186 In a closer look, the key feature of the *Recompression* cycle to enable higher efficiencies is a significant reduction

187 of exergy losses in the recuperator, as highlighted by Angelino originally [43]. This is thanks to the balanced heat
188 capacities on both sides of this heat exchanger, brought about by the lower mass flow rate on the low pressure side of it
189 (with higher specific heat at constant pressure c_p). In order to achieve this balance, the compression process is split in
190 two parallel streams which experience compression with the same pressure ratio but different inlet temperatures and
191 flow rates, Figure 2(c). The outcome is a higher temperature at the inlet to the primary heat exchanger, Figure 3(c),
192 which translates into a higher thermal efficiency of the cycle.

193
194 On the negative side, compression work increases in a *Recompression* layout, inasmuch as part of the compres-
195 sion process takes place in gaseous state, thereby reducing the specific work W_s of the cycle. Compensating for this is
196 actually the main driver of the *Precompression* cycle as explained by the results in Figures 3(c-d) and 2. With respect
197 to a reference *Recuperated Rankine* layout, the *Precompression* layout enables a significant reduction in turbine outlet
198 pressure p_3 and this brings about a parallel increase of specific work and thermal efficiency. This is so because the ad-
199 ditional work of the precompressor installed in between the recuperators, see Figure 2(b), is lower than the additional
200 expansion work obtained from the turbine [43]. The gain in specific work does however not translate into a similar
201 efficiency gain due to the lower turbine outlet temperature that limits the potential for internal heat recovery at the
202 high temperature recuperator, Figure 3(c). Yet, the slightly higher heat supply to the cycle is more than compensated
203 for by the higher specific work, what has a positive impact on thermal efficiency overall.

204
205 The results shown in this section confirm that, regardless of cycle layout and turbine inlet temperature: 1) the min-
206 imum molar fraction of dopant (in the range studied) always yields maximum thermal efficiency; and 2) the highest
207 specific work is obtained for the highest concentration of SO_2 . A lower SO_2 content also leads to higher temperatures
208 at the inlet to the primary heat exchanger (Figure 3b,c) and, therefore, lower temperature rise across this component
209 (ΔT_{PHE}). This has a direct impact on the temperature rise available in the solar receiver (i.e., operating temperature
210 range of molten salts) and, therefore, on the size and cost of the Thermal Energy Storage system and of the entire
211 Concentrated Solar Power plant [11]. Unfortunately, the compromise between these three figures of merit in a prac-
212 tical application (i.e., the composition of the optimum mixture) cannot be unequivocally identified without an overall
213 techno-economic assessment based on capital cost and Levelised Cost of Energy, in addition to other considerations
214 discussed in section 2. For instance, a lower content of SO_2 is interesting from social and environmental standpoints,
215 due to safety concerns regarding SO_2 leaking out from the system (highly irritant fluid), and it could also help reduce
216 the higher maintenance costs that could be caused by corrosion. But at the same time, a lower SO_2 content would
217 lead to a lower critical temperature of the mixture, thus a more challenging design and operation of the compression
218 device (pump).

219

[‡]This parameter is representative of the minimum cycle pressure, which is now allowed to vary in order to maximise thermal efficiency [18].

220 Unfortunately, such a complex analysis cannot be carried out at present, given the early stage of development of
 221 some of the key components in the plant (not only major components but also Balance of Plant equipment), the lack
 222 of suitable cost-estimation tools and data to properly address the socio-environmental impact of this technology by
 223 means of LCA analysis[§]. This is why thermal efficiency is selected as the primary driver in this paper and why the
 224 optimum molar content of Sulphur Dioxide depends directly on the assumption made about the difference between
 225 T_{cr} and T_{min} , regardless of cycle layout and turbine inlet temperature. Using this approach, a 30% SO₂ content is
 226 selected for the conservative case of $\Delta T_{gap}=30^{\circ}\text{C}$, whilst this content is reduced to 20% SO₂ if $\Delta T_{gap}=15^{\circ}\text{C}$. For the
 227 sake of simplicity, and due to the very similar thermal performances presented by these two mixtures, the authors have
 228 decided to consider only the more conservative case in Sections 4.2, 4.3 and 5.

230 4.2. Influence of the performance of turbomachinery and recuperators

231 In this section, the effect of component efficiency on cycle performance is investigated for a *Recompression* cycle
 232 working on 70%CO₂-30%SO₂ and 700°C turbine inlet temperature. The isentropic efficiency of each turbomachine
 233 (pump, compressor and turbine) is varied, one at a time, from 80% to 100% in 1% incremental steps and the resulting
 234 impact on cycle performance is shown in Figure 4. As expected, turbine efficiency has the strongest impact on cycle
 235 efficiency, leading to a 10% η_{th} drop when changing from 93% to 80%. Despite this, 50% thermal efficiency can still
 236 be attained for turbine efficiencies $\geq 90\%$, a specification that is not uncommon in literature [5]. Furthermore, it is
 237 worth noting that thermal efficiency is always higher than 50% for any value of pump and compressor efficiency in
 238 the aforecited range.

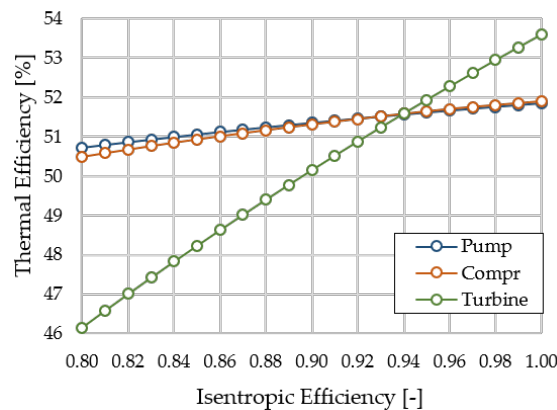


Figure 4: Sensitivity of cycle efficiency to isentropic efficiency of turbomachinery. Results apply to a *Recompression* cycle working on 70%CO₂-30%SO₂ and 700°C turbine inlet temperature.

[§]All these tasks are currently under development by the SCARABEUS consortium.

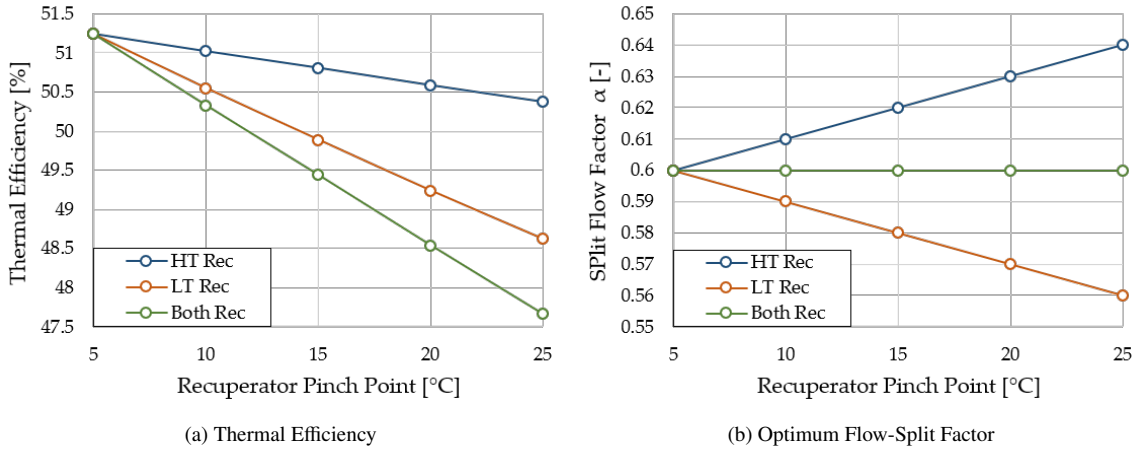


Figure 5: Sensitivity of cycle efficiency to recuperator pinch point (a), along with the corresponding values of flow-split factor (b). Results apply to a *Recompression* cycle working on 70%CO₂-30%SO₂ and 700°C.

240 The effect of recuperator performance is presented in Figure 5. This plot reports the maximum thermal efficiency
 241 attainable and the corresponding flow-split factor of a *Recompression* cycle when the pinch points of the recuperators
 242 take values between 5 and 25°C. Results are provided for the individual and joint variation of pinch points in the high
 243 and low temperature recuperators, confirming that the influence of the low temperature recuperator is dominant (LT
 244 Rec in Figure 2). A 20°C rise in $\Delta T_{pp,LTRec}$ leads to $\Delta \eta_{th} > 5\%$ whereas the same variation in $\Delta T_{pp,HTRec}$ yields
 245 $\Delta \eta_{th} \approx 1.7\%$.

246
 247 Another interesting feature in Figure 5 is the symmetrical trend of the optimum flow-split factor (α), defined as the
 248 fraction of fluid flowing across the Low-Temperature Recuperator (stations 1-2-3 in Figure 2(c)). In order to maximise
 249 thermal efficiency, α decreases when the performance of LT Rec deteriorates (i.e., when $\Delta T_{pp,LTRec}$ increases), whilst
 250 it increases when this performance drop takes place in the HT Rec. These two effects cancel each other out when
 251 the ΔT_{pp} of the two recuperators vary simultaneously: in this case, the optimum flow-split factor remains virtually
 252 constant.

253 4.3. Comparison with other dopants

254 Previous sections have shown the good performance of the transcritical *Recompression* cycle applied to CSP plants
 255 (i.e., to the corresponding boundary conditions). According to the results presented, thermal efficiencies of $\sim 45\%$ at
 256 550°C and $> 51\%$ at 700°C seem possible when working with 30% SO₂ content. This potential, corresponding to
 257 the more conservative assumption of ΔT_{gap} , is now compared against other dopants that were considered in previous
 258 publications of the same authors, within the SCARABEUS project, and also against pure CO₂. Figure 6 shows the
 259 thermal efficiency, specific work and temperature rise across the primary heat exchanger of the three cycle configura-
 260 tions considered in earlier sections for each working fluid. Solid bars refer to 550°C whilst striped bars correspond

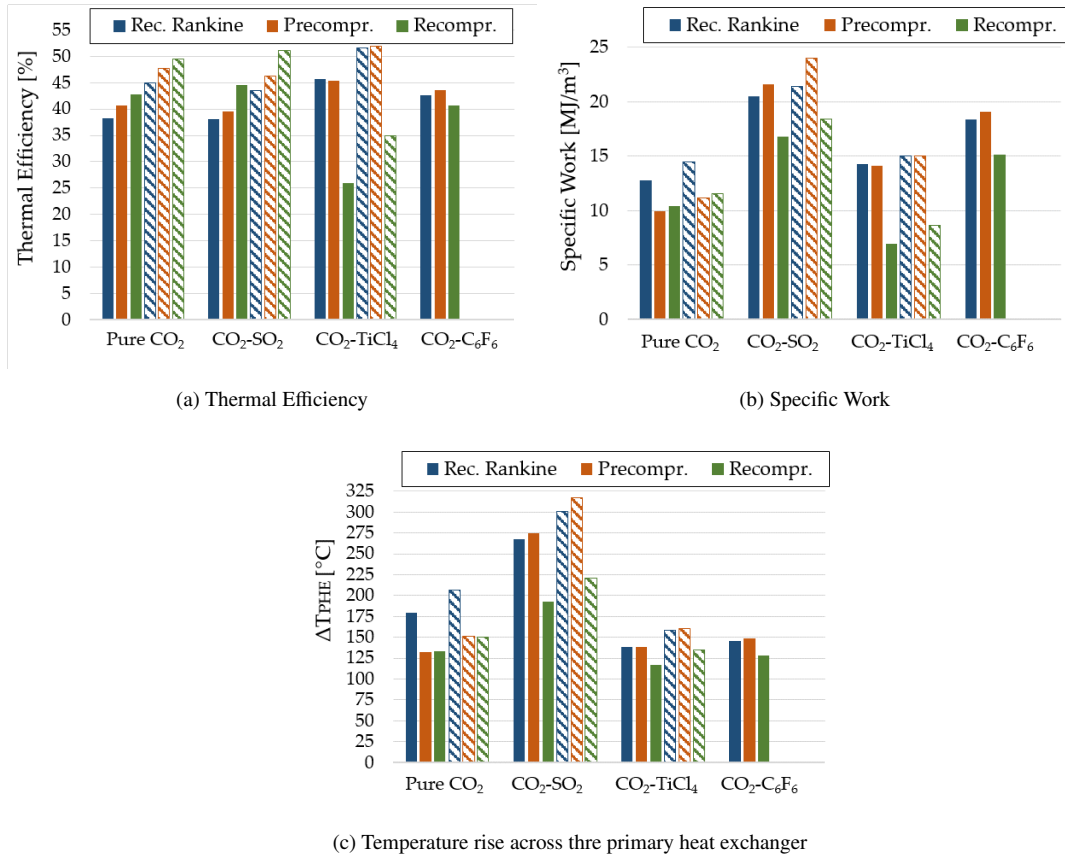


Figure 6: Performance comparison for different working mixtures, cycle layouts and turbine inlet temperatures. Solid and striped bars refer to 550°C and 700°C respectively. Results for CO₂-C₆F₆ are not reported at 700°C, due to thermal stability issues.

261 to 700°C. The composition of the working mixture is case-sensitive: 85%CO₂-15%C₆F₆ and 83%CO₂-17%TiCl₄ for
 262 both *Recuperated Rankine* or *Precompression* layouts and 90%CO₂-10%C₆F₆ and 85%CO₂-15%TiCl₄ for the *Re-*
 263 *compression* cycle. Specific work is expressed in volumetric terms ($W_{s,VOL}$) in order to account for the impact of
 264 the largely different density of the working fluids on the size of components. Finally, it is to note that the results
 265 for CO₂-C₆F₆ are provided for the lower temperature level only, given that these mixtures have experienced thermal
 266 degradation at temperatures higher than 625°C during the experimental activities carried out by the SCARABEUS
 267 consortium (see Table 2).

268
 269 The results in Figure 6 confirm that the three CO₂ mixtures yield higher performance than pure CO₂. The thermal
 270 efficiency gains experienced at 550°C are in the order of 7.5, 4.5 and 1.8 percentage points when compared to the sim-
 271 ple *Recuperated Rankine*, *Precompression* or *Recompression* cycles respectively, and slightly lower if the higher TIT
 272 of 700°C is considered (around 6.7, 4.3 and 1.7). Nevertheless, it is also true that the mixtures exhibit largely different
 273 behaviour when combined with different cycle layouts. For instance, CO₂-C₆F₆ performs best in a *Precompression*

274 layout ($\eta_{th} \approx 43.6\%$ at 550°C), whilst the potential of $\text{CO}_2\text{-TiCl}_4$ is fully exploited by the *Recuperated Rankine* layout
275 (η_{th} in the order of 45.7% and 51.5% for 550°C and 700°C respectively)[¶]. Both mixtures have rather poor performance
276 when coupled to a *Recompression* cycle, this being the reason why this cycle layout was dismissed in previous works
277 [44]; interestingly, this particular cycle turns out to be the best option for $\text{CO}_2\text{-SO}_2$ mixtures. In this and other aspects
278 (for instance, some thermodynamic properties, Section 2), $\text{CO}_2\text{-SO}_2$ mixtures and pure CO_2 behave very similarly
279 (Figure 6(a)); the reasons for this are discussed in the next section.

280
281 From the results presented in this section, it is concluded that the two most interesting cycle options for the
282 SCARABEUS concept are the *Recuperated Rankine* cycle working on $\text{CO}_2\text{-TiCl}_4$ and the *Recompression* cycle work-
283 ing on $\text{CO}_2\text{-SO}_2$, closely followed by the *Precompression* layout with $\text{CO}_2\text{-C}_6\text{F}_6$ but only for the lower turbine inlet
284 temperature. This ranked list is based on thermal efficiency only and, when $W_{s,VOL}$ and ΔT_{PHE} are also included in the
285 comparison, the benefits attained by $\text{CO}_2\text{-SO}_2$ mixtures become larger. At 550°C , the proposed *Recompression* cycle
286 enables both $W_{s,VOL}$ and ΔT_{PHE} significantly higher than those obtained by TiCl_4 (15% and 28.4% respectively), with
287 an expected positive impact on the size and cost of the components of both power block and Thermal Energy Storage
288 system; and the difference becomes even larger at higher TIT. A *Recompression* cycle with $\text{CO}_2\text{-SO}_2$ presents 13.7%
289 lower $W_{s,VOL}$ than C_6F_6 , but this is compensated for by the higher η_{th} (1 percentage point) and the almost 30% higher
290 ΔT_{PHE} ; in both cases, a *Recompression* cycle running on $\text{CO}_2\text{-SO}_2$ seems to ensure the best compromise between
291 the three figures of merit. Finally, the superb performance of $\text{CO}_2\text{-SO}_2$ mixtures in a *Precompression* cycles is worth
292 noting. This configuration attains $W_{s,VOL}$ and ΔT_{PHE} that are 35% and 50% higher than what can be achieved by
293 $\text{CO}_2\text{-TiCl}_4$ mixtures, regardless of cycle layout, and over 11% and 46% higher than when using $\text{CO}_2\text{-C}_6\text{F}_6$.

294

295 5. Applicability of transcritical *Recompression* cycles running on CO_2 mixtures

296 The previous section has shown that the performance of the transcritical *Recompression* cycle depends strongly on
297 the nature of the dopant considered, yielding thermal efficiencies that range from 25% to 45% at 550°C turbine inlet
298 temperature and from 35% to 51% at 700°C . In order to investigate this further and to assess the actual applicability
299 of this cycle, the thermal efficiencies for different molar fractions of C_6F_6 , TiCl_4 and SO_2 are compared in Figure
300 7, along with the temperature glide of the mixtures considered and the corresponding flow-split factors (α). In this
301 section, the analysis is limited to the lower temperature in order to enable the comparison for the entire set of dopants
302 (C_6F_6 is thermally stable up to 625°C only, see Table 2).

303

[¶]As a matter of fact, the *Precompression* cycle enables slightly higher η_{th} than the simple recuperated cycle for this mixture but the gain is so limited that the use of a more complex layout is not justified [18].

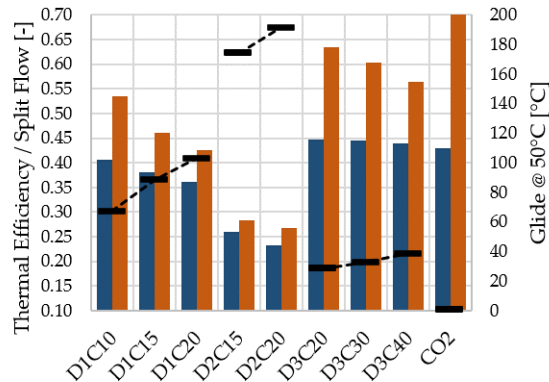


Figure 7: Thermal efficiency (blue bar), temperature glide (black marker) and flow-split factor (brown bar) of a transcritical *Recompression* cycle operating on different CO₂ mixtures. Turbine inlet temperature is set to 550°C.

304 Figure 7 reveals that higher thermal efficiencies are attained by working mixtures with a smaller temperature glide,
 305 as this yields a narrower two-phase region in Figure 1 providing the recompressor with more flexibility to fully ex-
 306 ploit the features of the *Recompression* cycle. For those mixtures with larger glides (C₆F₆ and TiCl₄), the recuperator
 307 outlet (low-pressure side) falls inside the two-phase region, what is certainly positive in *Recuperated Rankine* cycles
 308 because it leads to a lower condenser duty and a higher potential for heat recovery [18, 44]. Unfortunately, this is
 309 also problematic in terms of the actual practicability of the *Recompression* layout because, in order to successfully
 310 operate this cycle, the inlet to the recompressor (station 9 in Figure 2) must be in superheated state and this implies
 311 much lower flow-split factors (0.4-0.55 for C₆F₆, <0.3 for TiCl₄). These low values of α are detrimental for thermal
 312 efficiency as they imply an inevitable performance drop of the low-temperature recuperator. As opposed to this, the
 313 narrow two-phase region of CO₂-SO₂ mixtures (small temperature glide) enables having superheated steam at the in-
 314 let to the recompressor with suitable flow-split factors and this is very beneficial for the cycle from a thermodynamic
 315 standpoint, in particular for heat recovery in the low-temperature recuperator, and it leads to significantly higher ther-
 316 mal efficiencies.

317
 318 For CO₂-SO₂ mixtures, the optimum flow-split factor is 0.60, very close to the cycle using pure Carbon Dioxide
 319 with the same boundary conditions: 0.71 [18]. This confirms the similar thermodynamic behaviour of CO₂-SO₂ and
 320 pure CO₂, which can also be observed in the heat and mass balance provided in Tables 5 and 6 where the corresponding
 321 densities and compressibility factors are also fairly similar. The only exceptions to this are stations 1 and 2, pump
 322 inlet and outlet sections, whose significantly lower Z in the CO₂-SO₂ case is brought about by fluid condensation.
 323 This is the main reason for the enhanced performance of CO₂-SO₂ mixtures as compared to pure CO₂, and confirms
 324 the validity of the SCARABEUS concept.

Table 5: Heat and mass balance of the *Recompression* cycle with pure CO₂. Compressor and turbine inlet temperatures are 50°C and 700°C. Maximum cycle pressure is 250 bar. Station numbers as per Figure 2 (note that the cycle is fully supercritical).

Cycle Station	T [°C]	P [bar]	h [kJ/kg]	s [kJ/kgK]	\dot{m} [kg/s]	ρ [kg/m ³]	Z [-]
1	50.00	102.0	-128.3	-1.18	751	408.6	0.409
2	102.7	250.0	-95.47	-1.17	751	576.1	0.611
3	193.4	246.3	68.37	-0.77	751	330.3	0.846
4	193.7	246.3	68.69	-0.77	1061	330.0	0.846
5	549.2	242.7	525.4	-0.04	1061	149.7	1.044
6	700.0	239.1	716.1	0.18	1061	123.3	1.054
7	585.8	105.1	580.2	0.19	1061	63.67	1.017
8	198.7	104.1	123.5	-0.51	1061	128.0	0.912
9	107.7	103.0	7.52	-0.79	1061	186.5	0.768
10	194.2	246.3	69.46	-0.77	310	329.3	0.847

Table 6: Heat and mass balance of the *Recompression* cycle with 70%CO₂ - 30%SO₂ (D3C30). Pump and turbine inlet temperatures are set to 50°C and 700°C. Maximum cycle pressure is 250 bar. Station numbers as per Figure 2.

Cycle Station	T [°C]	P [bar]	h [kJ/kg]	s [kJ/kgK]	\dot{m} [kg/s]	ρ [kg/m ³]	Z [-]
1	50.00	68.53	-7520.6	-1.118	464.1	840.1	0.152
2	74.54	250.0	-7497.4	-1.110	464.1	927.1	0.467
3	206.4	246.3	-7247.2	-0.493	464.1	392.8	0.787
4	206.5	246.3	-7246.9	-0.493	769.7	392.6	0.787
5	478.2	242.6	-6909.7	0.072	769.7	190.2	1.021
6	700.0	238.9	-6655.7	0.371	769.7	140.4	1.052
7	534.2	69.93	-6827.1	0.387	769.7	51.87	1.005
8	211.5	69.23	-7164.4	-0.144	769.7	94.96	0.905
9	83.77	68.53	-7315.3	-0.508	769.7	180.1	0.642
10	206.7	246.3	-7246.6	-0.492	305.6	392.2	0.787

325 The results presented in this section confirm that the adoption of CO₂-SO₂ mixtures in a *Recompression* cycle is
326 interesting for several reasons. First and foremost, it enables thermal efficiencies that are 2 percentage points higher
327 than the efficiency attained by pure CO₂ for the same cycle layout and boundary conditions. Second, the similar
328 thermodynamic behaviour of the working fluid enables capitalising the knowledge and technology developed for pure
329 supercritical CO₂ cycles in recent years (thereby avoiding large deviations from the current research and develop-
330 ment pathway of the industry and scientific community). In fact, given that even the cycle layout that yields best
331 performance is very likely the same (*Recompression*), it is foreseen that adopting the same part-load and off-design

operating strategies as in a sCO₂ cycle would be possible. Of course, this must be confirmed by specific analysis in later stages of this research.

5.1. Influence of minimum cycle temperature

In this last section, the influence of minimum cycle temperature on the optimum molar fraction of Sulphur Dioxide is investigated, with the aim to confirm the results obtained in previous sections and to assess the potential of CO₂-SO₂ cycles at high ambient temperatures. To this end, Figure 8 illustrates a sensitivity analysis of cycle performance to minimum cycle temperature, when this parameter is varied between 30°C and 60°C; results apply to a *Recompression* cycle running on different CO₂/SO₂ mixtures at 700°C. Solid lines and black markers in the plot refer to cases for which the minimum temperature glide condition is met ($\Delta T_{gap} \geq 30^\circ\text{C}$), whilst dotted lines and white markers refer to cases where $\Delta T_{gap} < 30^\circ\text{C}$. It is worth noting that the mixture with 10% SO₂ content ($y=0.1$ in Figure 8) does never comply with this condition $\Delta T_{gap} \geq 30^\circ\text{C}$ whereas the mixture with 20% SO₂ satisfies this condition for minimum cycle temperatures lower than 35°C only. Finally, a dashed line with triangular markers provides the performance of a reference *Recompression* cycle running on pure CO₂ [18].

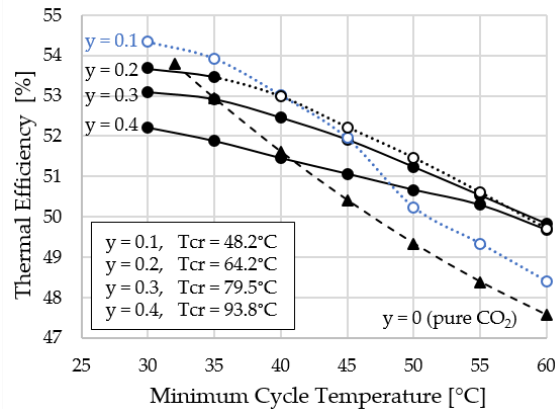


Figure 8: Sensitivity analysis of cycle performance to minimum cycle temperature. Results are shown for CO₂-SO₂ mixtures with molar fractions of SO₂ between 10% and 40%.

Figure 8 confirms that the proposed utilisation of CO₂ mixtures is of interest at high ambient temperatures only. At low minimum cycle temperatures, close to the critical temperature of Carbon Dioxide, the performance of a *Recompression* cycle operating on pure CO₂ ($y = 0$) is similar or even higher than when mixtures are used. On the contrary, at 40°C (equivalent to ambient temperatures of around 25-30°C), adding 30% SO₂ yields a 1 percentage point increase in thermal efficiency with respect to the reference case using pure CO₂. If the minimum cycle temperature increases to 45°C, which is a very likely situation in warm environments, the thermal efficiency difference between pure CO₂ cycles and a cycle with 30% CO₂ content is 1.5 percentage points. Finally, at 60°C, corresponding to extreme ambient

354 temperatures and air-cooled cycles, the thermal efficiency gain is as high as 2 percentage points.

355

356 Another very interesting conclusion from Figure 8 is that, regardless of ambient temperature, the optimum mix-
357 ture results to be the one with the minimum Sulphur Dioxide content still complying with the constraint set on the
358 temperature difference between the critical temperature and the temperature at pump inlet (ΔT_{gap}). Furthermore, the
359 impact of SO_2 content on performance is larger at low ambient temperature and decreases at higher temperatures, as
360 seen from the distance between lines of constant y in the plot. This information will be combined with other techno-
361 economic, operational and socio-environmental benefits associated to a lower or higher content of Sulphur Dioxide in
362 the future.

363

364 Overall, this last set of results confirms not only the conceptual interest of the SCARABEUS concept but, also,
365 its flexibility and tailorability. Indeed, the plot in Figure 8 suggests that it is possible to produce a mixture whose
366 composition is optimised for a given set of boundary and operating conditions, not only for a particular plant site
367 but also to account for seasonal variations at a given location. This latter adaptability would however require the
368 ability to control the composition of the mixture in real-time in order to always attain the maximum efficiency for the
369 time-specific ambient temperature; the technical feasibility of this is uncertain since reducing the SO_2 content of the
370 mixture is not a trivial procedure to be performed daily. Another caveats to this would be the impact of the variable
371 composition of the working fluid on the performance of major components like turbomachines and heat exchangers.

372

373 6. Conclusions

374 This paper has analysed the utilisation of mixtures composed of Carbon and Sulphur Dioxides in transcritical
375 *Recompression* cycles, in order to assess the potential of this technology in Concentrated Solar Power plants operating
376 at high ambient temperature. This solution has been compared against similar cycles using pure CO_2 or mixtures of
377 Carbon Dioxide with either Hexafluorobenzene (C_6F_6) or Titanium Tetrachloride ($TiCl_4$), as already proposed by the
378 authors in past works. Two different turbine inlet temperatures have been considered: $550^\circ C$, representative of state-
379 of-the-art Concentrated Solar Power plants with central receiver, and $700^\circ C$, representative of next generation CSP
380 technology. For the sake of comparison, two other cycle layouts have also been considered: *Recuperated Rankine* and
381 *Precompression*.

382 The following conclusions are drawn from this work:

- 383 • The *Recompression* cycle is the most efficient cycle option to exploit the thermodynamic potential of CO_2 - SO_2
384 mixtures, attaining thermal efficiencies that are 18% and 11% higher than when these mixtures are used in
385 *Recuperated Rankine* and *Precompression* cycles respectively. This is brought about by the particular pressure-
386 temperature envelopes presented by CO_2 - SO_2 , which are significantly narrower than those of C_6F_6 and $TiCl_4$.

- 387 • The *Recompression* cycle enables thermal efficiencies higher than 51% at minimum cycle temperature as high
388 as 50°C running on CO₂-SO₂, hence stepping forward as a promising alternative for next-generation CSP plants.
389 Furthermore, this mixture enables thermal efficiencies higher than 50% even with minimum cycle temperatures
390 as high as 60°C.
- 391 • From a thermodynamic standpoint, Sulphur Dioxide presents several beneficial features with respect to C₆F₆
392 and TiCl₄, with a globally better compromise between the three main figures of merit considered: thermal
393 efficiency, specific work and temperature rise across primary heat exchanger. Moreover, SO₂ presents high
394 thermal stability and it is not flammable.
- 395 • The superior performance of the *Recompression* cycle running on CO₂-SO₂ with respect to the same cycle using
396 pure CO₂ is evident at high minimum cycle temperatures, enabling gains in the order of 2 percentage points,
397 37% and 30% for η_{th} , W_s and ΔT_{PHE} respectively. The benefits at low turbine inlet temperatures are marginal.
- 398 • The molar content of Sulphur Dioxide has a very weak effect on cycle performance when ambient temperatures
399 are high, as long as condensation of the working fluid is enabled ($y \geq 0.2$), whilst the influence becomes stronger
400 at lower temperatures.
- 401 • Overall, the *Recompression* cycle operated with 20%-30%(v) SO₂ content yields the most balanced performance
402 for the boundary conditions that are typical of CSP facilities. However, the identification of the optimum
403 mixture composition depends on a thorough multi-objective optimisation based on thermo-economic and LCA
404 analyses. The authors are currently working on this as part of the SCARABEUS project.

405 Nomenclature

406 α	Split Flow Factor [-]
407 ΔP_{HX}	HX Pressure drop [%]
408 ΔT_{gap}	Difference between T_{cr} and T_{min} [°C]
409 ΔT_{PHE}	Temperature rise across PHE [%]
410 ΔT_{pp}	Minimum temperature difference in HX (pinch point) [°C]
411 \dot{m}	Mass flow [kg/s]
412 η_{is}	Isentropic Efficiency [%]
413 η_{th}	Cycle Thermal Efficiency [%]
414 ρ	Specific Mass [kg/m ³]

415	<i>CSP</i>	Concentrated Solar Power
416	<i>h</i>	Enthalpy [J/kg]
417	<i>HTRec</i>	High Temperature Recuperator
418	<i>LCA</i>	Life Cycle Assessment
419	<i>LTRec</i>	Low Temperature Recuperator
420	<i>MW</i>	Molar Weight [kg/kmol]
421	<i>P_{cr}</i>	Critical Pressure [bar]
422	<i>P_{max}</i>	Maximum Cycle Pressure [bar]
423	<i>PHE</i>	Primary Heat Exchanger
424	<i>PIT</i>	Pump Inlet Temperature [°C]
425	<i>pp</i>	Percentage point [%]
426	<i>s</i>	Entropy [J/kgK]
427	<i>sCO₂</i>	Supercritical Carbon Dioxide
428	<i>T_{cr}</i>	Critical Temperature [°C]
429	<i>T_{min}</i>	Cycle minimum temperature [°C]
430	<i>TIT</i>	Turbine Inlet Temperature [°C]
431	<i>W_{s,VOL}</i>	Specific Work - volumetric base [MJ/m ³]
432	<i>W_s</i>	Specific Work [kJ/kg]
433	<i>y</i>	Molar fraction of dopant [-]
434	<i>Z</i>	Compressibility Factor [-]

435 **Acknowledgements**

436 The SCARABEUS project has received funding from the European Union's Horizon 2020 research and inno-
437 vation programme under grant agreement N°814985. The University of Seville is also gratefully acknowledged for
438 supporting this research through its Internal Research Programme (Plan Propio de Investigación), under contract No
439 2019/00000359. Last but not least, the regional government of Andalusia (Junta de Andalucía) is gratefully ac-
440 knowledged for sponsoring the contract of Pablo Rodríguez de Arriba under the Programme for Youth Employment
441 2014-2020 (Phase 4).

References

- [1] F. Crespi, G. Gavagnin, D. Sánchez, G. Martínez, Supercritical carbon dioxide cycles for power generation: a review, *Applied Energy* 195 (2017) 152–183. doi:<https://doi.org/10.1016/j.apenergy.2017.02.048>.
- [2] T. Neises, C. Turchi, Supercritical carbon dioxide power cycle design and configuration optimization to minimize levelized cost of energy of molten salt power towers operating at 650°C, *Solar Energy* 181 (2019) 27–36. doi:<https://doi.org/10.1016/j.solener.2019.01.078>.
- [3] A. Ameli, A. Afzalifar, T. Turunen-Saaresti, J. Backman, Centrifugal compressor design for near-critical point applications, *Journal of Engineering for Gas Turbines and Power* 141 (3). doi:<https://doi.org/10.1115/1.4040691>.
- [4] J. Lee, J. Lee, H. Yoon, J. Cha, Supercritical carbon dioxide turbomachinery design for water-cooled small modular reactor application, *Nuclear Engineering and Design* 270 (2014) 76–89. doi:<http://dx.doi.org/10.1016/j.nucengdes.2013.12.039>.
- [5] M. White, G. Bianchi, L. Chai, S. A. Tassou, A. Sayma, Review of supercritical CO₂ technologies and systems for power generation, *Applied Thermal Engineering* 185 (2021) 116447. doi:<https://doi.org/10.1016/j.applthermaleng.2020.116447>.
- [6] A. Romei, P. Gaetani, A. Giostri, G. Persico, The role of turbomachinery performance in the optimization of supercritical carbon dioxide power systems, *Journal of Turbomachinery* 142 (7) (2020) 071001. doi:<https://doi.org/10.1115/1.4046182>.
- [7] T. Neises, Steady-state off-design modeling of the supercritical carbon dioxide recompression cycle for concentrating solar power applications with two-tank sensible-heat storage, *Solar Energy* 212 (2020) 19–33. doi:<https://doi.org/10.1016/j.solener.2020.10.041>.
- [8] D. Alfani, M. Astolfi, M. Binotti, P. Silva, E. Macchi, Off-design performance of CSP plant based on supercritical CO₂ cycles, in: *AIP Conference Proceedings*, Vol. 2303, AIP Publishing LLC, 2020, p. 130001. doi:<https://doi.org/10.1063/5.0029801>.
- [9] M. Carlson, B. Middleton, C. Ho, Techno-economic comparison of solar-driven sCO₂ brayton cycles using component cost models baselined with vendor data and estimates, in: *Energy Sustainability*, Vol. 57595, American Society of Mechanical Engineers, 2017, p. V001T05A009. doi:<https://doi.org/10.1115/ES2017-3590>.
- [10] N. Weiland, B. Lance, S. Pidaparti, sCO₂ power cycle component cost correlations from DOE data spanning multiple scales and applications, in: *Turbo Expo: Power for Land, Sea, and Air*, Vol. 58721, American Society of Mechanical Engineers, 2019, p. V009T38A008. doi:<https://doi.org/10.1115/GT2019-90493>.
- [11] F. Crespi, D. Sánchez, T. Sánchez, G. Martínez, Capital cost assessment of concentrated solar power plants based on supercritical carbon dioxide power cycles, *Journal of Engineering for Gas Turbines and Power* 141 (7). doi:<https://doi.org/10.1115/1.4042304>.
- [12] C. Invernizzi, T. van der Stelt, Supercritical and real gas brayton cycles operating with mixtures of carbon dioxide and hydrocarbons, *Proceedings of the Institution of Mechanical Engineers, Part A: Journal of Power and Energy* 226 (5) (2012) 682–693. doi:<https://doi.org/10.1177/0957650912444689>.
- [13] M. Siddiqui, Thermodynamic performance improvement of recompression brayton cycle utilizing CO₂-C₇H₈ binary mixture, *Mechanics* 27 (3) (2021) 259–264. doi:[10.5755/j02.mech.28126](https://doi.org/10.5755/j02.mech.28126).
- [14] S. Baik, J. Lee, Preliminary study of supercritical CO₂ mixed with gases for power cycle in warm environments, in: *Turbo Expo: Power for Land, Sea, and Air*, Vol. 51180, American Society of Mechanical Engineers, 2018, p. V009T38A017. doi:<https://doi.org/10.1115/GT2018-76386>.
- [15] G. Manzoloni, M. Binotti, D. Bonalumi, C. Invernizzi, P. Iora, CO₂ mixtures as innovative working fluid in power cycles applied to solar plants. techno-economic assessment, *Solar Energy* 181 (2019) 530–544. doi:<https://doi.org/10.1016/j.solener.2019.01.015>.
- [16] *Supercritical CARBON dioxide/Alternative fluids Blends for Efficiency Upgrade of Solar power plants*, online, accessed May 12th 2021 (2019). URL <https://cordis.europa.eu/project/rcn/221766/factsheet/en>
- [17] M. Binotti, G. Di Marcoberardino, P. Iora, C. Invernizzi, G. Manzoloni, Scarabeus: Supercritical carbon dioxide/alternative fluid blends for efficiency upgrade of solar power plants, in: *AIP Conference Proceedings*, Vol. 2303, AIP Publishing LLC, 2020, p. 130002. doi:<https://doi.org/10.1063/5.0028799>.
- [18] F. Crespi, P. Rodríguez de Arriba, D. Sánchez, A. Ayub, G. Di Marcoberardino, C. Invernizzi, G. Martínez, P. Iora, D. Di Bona, M. Binotti,

- 485 G. Manzoloni, Thermal efficiency gains enabled by using CO₂ mixtures in supercritical power cycles, *Energy* (2021) 121899doi:<https://doi.org/10.1016/j.energy.2021.121899>.
- 486
- 487 [19] D. Bonalumi, S. Lasala, E. Macchi, CO₂-TiCl₄ working fluid for high-temperature heat source power cycles and solar application, *Renewable*
- 488 *Energy* 147 (2020) 2842–2854. doi:<https://doi.org/10.1016/j.renene.2018.10.018>.
- 489 [20] G. Di Marcoberardino, E. Morosini, G. Manzoloni, Preliminary investigation of the influence of equations of state on the performance of
- 490 CO₂+C₆F₆ as innovative working fluid in transcritical cycles, *Energy* (2021) 121815doi:[https://doi.org/10.1016/j.energy.2021.](https://doi.org/10.1016/j.energy.2021.121815)
- 491 [121815](https://doi.org/10.1016/j.energy.2021.121815).
- 492 [21] P. Tafur-Escanta, R. Valencia-Chapi, I. López-Paniagua, L. Coco-Enríquez, J. Muñoz-Antón, Supercritical CO₂ binary mixtures for re-
- 493 compression brayton sCO₂ power cycles coupled to solar thermal energy plants, *Energies* 14 (13). doi:[https://doi.org/10.3390/](https://doi.org/10.3390/en14134050)
- 494 [en14134050](https://doi.org/10.3390/en14134050).
- 495 [22] L. Wang, L. Pan, J. Wang, D. Chen, Y. Huang, W. Sun, L. Hu, Investigation on the effect of mixtures physical properties on cycle efficiency in
- 496 the CO₂-based binary mixtures brayton cycle, *Progress in Nuclear Energy* (2021) 104049doi:[https://doi.org/10.1016/j.pnucene.](https://doi.org/10.1016/j.pnucene.2021.104049)
- 497 [2021.104049](https://doi.org/10.1016/j.pnucene.2021.104049).
- 498 [23] S. Rath, E. Mickoleit, U. Gampe, C. Breitkopf, A. Jäger, Study of the influence of additives to CO₂ on the performance parameters of a sCO₂-
- 499 cycle, in: *Proceedings of 4th European sCO₂ Conference for Energy Systems, sCO₂-Flex Project, 2021*. doi:10.17185/dupublico/
- 500 [73965](https://doi.org/10.17185/dupublico/73965).
- 501 [24] O. Aqel, M. White, M. Khader, A. Sayma, Sensitivity of transcritical cycle and turbine design to dopant fraction in CO₂-based working fluids,
- 502 *Applied Thermal Engineering* 190 (2021) 116796. doi:<https://doi.org/10.1016/j.applthermaleng.2021.116796>.
- 503 [25] *Evaluations of the joint FAO/WHO expert committee on food additives (JECFA)*, online, accessed December 31th 2021 (1998).
- 504 URL <https://apps.who.int/food-additives-contaminants-jecfa-database/chemical.aspx?chemID=985>
- 505 [26] B. D. Horbaniuc, Refrigeration and air-conditioning, in: C. J. Cleveland (Ed.), *Encyclopedia of Energy*, Elsevier, New York, 2004, pp.
- 506 261–289. doi:<https://doi.org/10.1016/B0-12-176480-X/00085-1>.
- 507 [27] *PubChem, Compound Summary: Sulfur Dioxide*, online, accessed December 31th 2021 (2021).
- 508 URL <https://pubchem.ncbi.nlm.nih.gov/compound/Sulfur-dioxide>
- 509 [28] D. Kirk-Othmer, *Encyclopedia of Chemical Technology*, 4th edn., vol. 23 (2001). doi:10.1002/0471238961.
- 510 [29] *NFPA 704: Standard System for the Identification of the Hazards of Materials for Emergency Response*, online, accessed May
- 511 12th 2021 (2021).
- 512 URL [https://www.nfpa.org/codes-and-standards/all-codes-and-standards/list-of-codes-and-standards/detail?](https://www.nfpa.org/codes-and-standards/all-codes-and-standards/list-of-codes-and-standards/detail?code=704)
- 513 [code=704](https://www.nfpa.org/codes-and-standards/all-codes-and-standards/list-of-codes-and-standards/detail?code=704)
- 514 [30] A. S. of Heating, Refrigerating, A.-C. Engineers, *ASHRAE Handbook: Refrigeration systems and applications*, American Society of Heating,
- 515 *Refrigerating and Air Conditioning Engineers*, 1986.
- 516 [31] L. Hanson, L. Ritter, Toxicity and safety evaluation of pesticides, in: R. Krieger (Ed.), *Hayes' Handbook of Pesticide Toxicology (Third*
- 517 *Edition)*, third edition Edition, Academic Press, New York, 2010, pp. 333–336. doi:<https://doi.org/10.1016/C2009-1-03818-0>.
- 518 [32] C. Invernizzi, Closed power cycles, *Lecture Notes in Energy* 11. doi:10.1007/978-1-4471-5140-1.
- 519 [33] P. Bombarda, C. Invernizzi, Binary liquid metal–organic rankine cycle for small power distributed high efficiency systems, *Proceedings of*
- 520 *the Institution of Mechanical Engineers, Part A: Journal of Power and Energy* 229 (2) (2015) 192–209. doi:10.1177/0957650914562094.
- 521 [34] N. Vannerberg, T. Sydberger, Reaction between SO₂ and wet metal surfaces, *Corrosion Science* 10 (1) (1970) 43–49.
- 522 [35] Y. Zeng, K. Li, Influence of SO₂ on the corrosion and stress corrosion cracking susceptibility of supercritical CO₂ transportation pipelines,
- 523 *Corrosion Science* 165 (2020) 108404. doi:10.1016/j.corsci.2019.108404.
- 524 [36] *NET Power's clean energy demonstration plant, La Porte, Texas*, online, accessed May 12th 2021 (2016).
- 525 URL <https://www.power-technology.com/projects/net-powers-clean-energy-demonstration-plant-la-porte-texas/>
- 526 [37] G. Cui, Z. Yang, J. Liu, Z. Li, A comprehensive review of metal corrosion in a supercritical co₂ environment, *International Journal of*
- 527 *Greenhouse Gas Control* 90 (2019) 102814. doi:<https://doi.org/10.1016/j.ijggc.2019.102814>.

- 528 [38] K. Li, Y. Zeng, J. Luo, Corrosion of SS310 and Alloy 740 in high temperature supercritical CO₂ with impurities H₂O and O₂, Corrosion
529 Science 184 (2021) 109350. doi:<https://doi.org/10.1016/j.corsci.2021.109350>.
- 530 [39] G. Obulan Subramanian, S. H. Kim, J. Chen, C. Jang, Supercritical-CO₂ corrosion behavior of alumina- and chromia-forming heat resistant
531 alloys with Ti, Corrosion Science 188 (2021) 109531. doi:<https://doi.org/10.1016/j.corsci.2021.109531>.
- 532 [40] C. Coquelet, A. Valtz, P. Arpentinier, Thermodynamic study of binary and ternary systems containing CO₂+ impurities in the context of CO₂
533 transportation, Fluid Phase Equilibria 382 (2014) 205–211. doi:<https://doi.org/10.1016/j.fluid.2014.08.031>.
- 534 [41] [Thermoflow Inc, Thermoflow suite - Thermoflex software](#), online, accessed May 12th 2021 (2021).
535 URL [https://www.thermoflow.com/products/\\$_generalpurpose.html](https://www.thermoflow.com/products/$_generalpurpose.html)
- 536 [42] [Aspen plus - leading process simulator software](#), online, accessed May 12th 2021 (2011).
537 URL <https://www.aspentech.com/en/products/engineering/aspen-properties>
- 538 [43] G. Angelino, Real gas effects in carbon dioxide cycles 79832. doi:<https://doi.org/10.1115/69-GT-102>.
- 539 [44] F. Crespi, G. Martínez, P. Rodríguez de Arriba, D. Sánchez, F. Jiménez-Espadafor, Influence of working fluid composition on the optimum
540 characteristics of blended supercritical carbon dioxide cycles, in: Proceedings of ASME Turbo Expo, American Society of Mechanical
541 Engineers, 2021. doi:[10.1115/GT2021-60293](https://doi.org/10.1115/GT2021-60293).

542 **Appendix A. Influence of different EoS on Cycle Performance**

543 This section investigates the influence of using different Equations of state in the estimation of cycle thermal per-
544 formance. Peng-Robinson and PC-SAft equations of state has been taken into account in this comparison. These two
545 EoS have been found to be the ones providing the best fit with experimental data found in literature and produced
546 by SCARABEUS consortium experimental activity, led by University of Brescia and Politecnico di Milano. Unfor-
547 tunately, the complete set of results is still confidential, and it is going to be disclosed soon in another publication
548 developed by these institutions.

549
550 In order to consider a wider scenario, thus providing a more reliable comparison, three different Sulphur Dioxide
551 molar fractions have been taken into account – 20%, 30% and 40% – at two different turbine inlet temperature (550°C
552 and 700°C). All the results refer to a *Recompression* cycle, and correspond to a minimum cycle temperature of 50°C.

553
554 Table A.7 provides the values obtained for the four main figures of merit taken into account: thermal efficiency
555 (η_{th}), specific work – both mass-flow based (W_s) and volumetric flow-based ($W_{s,VOL}$)– and temperature rise across
556 primary heat exchanger (ΔT_{PHE}). Table A.8 presents the relative deviation of these values, obtained comparing the
557 results calculated with the two different equations of state. It results clear that both methodologies achieve very similar
558 results, with relative deviations ranging 0.04-1.5%, 0.34-3.7%, 0.19-3.43% and 0.21-1.03% for η_{th} , W_s , $W_{s,VOL}$ and
559 ΔT_{PHE} respectively. Furthermore, it is worth noting that the highest relative deviations refer to D3C40, the mixture
560 achieving the worst thermal performance and thus disregarded in the second part of the present paper. Considering
561 Sulphur Dioxide molar fractions ranging 20-30%, which are the most interesting according to the conclusions of
562 the present paper, maximum relative deviations results to be lower than 0.51%, 1.7%, 1.5% and 0.86% for η_{th} , W_s ,
563 $W_{s,VOL}$ and ΔT_{PHE} respectively. Therefore, the conclusion is that the influence of EoS on the estimation of cycle

Table A.7: Comparison of main cycle figures of merit obtained with Peng-Robinson and PC-Saft Equations of state

		TIT=550°C			TIT=700°C		
		D3C20	D3C30	D3C40	D3C20	D3C30	D3C40
Peng Robinson	η_{th} [%]	44.93	44.71	44.10	51.50	51.30	50.82
	W_s [kJ/kg]	94.19	100.3	103.2	122.3	130.3	135.3
	$W_{s,VOL}$ [MJ/m ³]	15.17	16.91	18.20	16.46	18.30	19.82
	ΔT_{PHE} [°C]	176.6	193.6	206.2	200.9	221.9	239.2
PC-SAFT	η_{th} [%]	44.95	44.48	43.45	51.50	51.14	50.40
	W_s [kJ/kg]	93.87	98.66	99.38	121.9	128.7	131.4
	$W_{s,VOL}$ [MJ/m ³]	15.14	16.68	17.58	16.35	18.03	19.22
	ΔT_{PHE} [°C]	178.11	194.0	204.5	201.6	221.6	236.7

Table A.8: Comparison of main cycle figures of merit obtained with PR and PC-Saft Eos: relative deviations Δ

		TIT=550°C			TIT=700°C		
		D3C20	D3C30	D3C40	D3C20	D3C30	D3C40
PR vs PC-SAFT	$\Delta(\eta_{th})$ [%]	0.04	0.51	1.47	0.00	0.31	0.83
	$\Delta(W_s)$ [%]	0.34	1.64	3.70	0.37	1.27	2.85
	$\Delta(W_{s,VOL})$ [%]	0.19	1.42	3.43	0.66	1.48	2.99
	$\Delta(\Delta T_{PHE})$ [%]	0.86	0.21	0.82	0.35	0.15	1.03

564 performance is minimum and, as a consequence, Peng-Robinson is a suitable EoS for the scope of the present paper.

565